Journal of Child & Adolescent Behavior

Bernal-Casas et al., J Child Adolesc Behav 2015, 3:5
DOI: 10.4172/2375-4494.1000251

Research Article Open Access

Discounting and VBM

Bernal-Casas D*, Ziegler G, Moutoussis M, Prabhu G and Dolan R

Department of Neurology, Wellcome Trust Centre for Neuroimaging, Institute of Neurology, University College London, London, UK

Abstract

Adolescence is a period of significant development in cognition, behavior, and the brain. Neural development during human adolescence involves highly coordinated and sequenced events, characterized by both progressive and regressive processes. In this study we were interested in the emergence of self-control as indexed by impulsivity, and the malleability to change their own preferences, a trait linked to pro-social behavior. We used a computationally derived measure of impulsivity based on an inter-temporal choice task, to examine how its trajectory over adolescence related to maturational morphological brain changes estimated by voxel based morphometry (VBM). We observed a global decrease in grey matter volume over the course of adolescence. Over and above these changes greater impulsivity as indexed in a higher self-discounting parameter was linked to greater grey matter volume within right dorsomedial prefrontal cortex (DMPFC). Likewise we observed that greater choice stochasticity, indexed by a higher decision-variability parameter (reflecting more "noisy" and "exploratory" choices) was linked to greater grey matter volume within bilateral dorsal striatum. We interpret these findings as suggestive that delay in cortical maturation within impulsivity-related brain areas, possibly linked to sluggish neuronal pruning, is a key mediator of impulsivity. Finally, the ability to shift towards other's behavior was positively correlated to grey matter volume within right dorsolateral prefrontal cortex (DLPFC). At first sight, this result seems to contradict previous findings but it does not; DLPFC undergoes a normal pruning across adolescence, however, the more grey matter participants had at the onset of the puberty, the more malleable were in shifting towards other's behaviour. This finding supports the idea that pro-social traits are developed in childhood.

Keywords: Discounting; Impulsivity; Structural MRI; VBM

Introduction

Adolescence is a transitional stage of significant psychological development and without doubt, maturational brain changes might map onto cognition and behaviors commonly observed in adolescents. Recent neuroimaging studies have showed specific changes in neural architecture, outlining trajectories of gray and white matter development, and differences in brain network function over puberty [1,2]. In this study we were interested in the emergence of impulsivity and pro-social behaviors in relation to structural brain maturation changes. Along the next lines we will review some studies that have attempted to provide reference curves for structural brain maturation in relation to impulsive and pro-social behaviors.

Impulsivity is a personality trait exhibited by healthy people, but excessive impulsivity is often linked to psychopathology. For over a while, impulsivity disorders have been associated with gray matter abnormalities in prefrontal cortex and striatal aspects [3-6]. One type of functional architecture has posited that striatal regions encode the current value of tangible rewards, whereas prefrontal regions represent more abstract rewards and long-term goals; although this view is certainly changing as we gain more knowledge [7]. In the striatum, ventral regions encode the value associated with the expected reward and the level of motivation induced by reward anticipation [8,9], whereas dorsal aspects are central for habit learning and habit-based control of instrumental behavior [10,11]. In the prefrontal cortex, ventromedial aspects represent the subjective value of rewards and goals and orchestrate goal-directed behavior [12-14], whereas dorsomedial aspects are invoked to address conflict and maintain motivation for challenges and goals over time [15-17].

However, despite all this knowledge, no studies have examined relations between brain structure and impulsivity over the course of adolescence and studies with participants in early or late puberty have not replicated findings [4,5]. For instance, colleagues demonstrated in boys [4] (age 12.08 ± 2.71 yrs.) a negative correlation between grey matter volume within right ventromedial prefrontal cortex and impulsivity derived measures using the Pediatric Behavior Scale (PBS). Few years later, [5] showed in young people (age 23.4 ± 4.3 yrs.) a positive correlation between grey matter volume within the same brain region and impulsivity scores measured with the Barratt Impulsivity Scale-11 (BIS) and a computerized delay discounting task. There is therefore a need to understand what is really happening over the course of adolescence.

Empathy is a psychological construct consisting of our ability not only to share emotions but also to exert cognitive control and perspective taking in our interactions with others. Models of empathy highlight two key aspects: cognitive empathy – predicting and understanding another's mental state by using cognitive processes, and affective empathy – experiencing an appropriate emotional response as a consequence of another's state [18,19]. Results from functional imaging studies converge in support of the hypothesis that an area of the temporoparietal junction (TPJ), near the superior temporal sulcus (STS), is consistently activated when making inferences about what another person believes, or when attributing a belief to another person [20-23]. Most of these studies indicate that this region has an important role in mentalizing and third-person perspective-taking, but not specifically for affective perspective-taking [23,24].

Along these lines, neuroimaging studies have investigated the way in which social brain regions, such as the TPJ, develop structurally

***Corresponding author:** Bernal-Casas D, Department of Neurology, Wellcome Trust Centre for Neuroimaging, Institute of Neurology, University College London, 12 Queen Square - London - WC1N 3BG, UK, Tel: ++44 (0) 20 3448 4362; Fax: ++44 (0) 20 7813 1420; E-mail: bernalgps@gmail.com

Received August 27, 2015; **Accepted** October 05, 2015; **Published** October 13, 2015

Citation: Bernal-Casas et al. (2015) Discounting and VBM. J Child Adolesc Behav 3: 251. doi:10.4172/2375-4494.1000251

Copyright: © 2015 Bernal-Casas et al. This is an open-access article distributed under the terms of the Creative Commons Attribution License, which permits unrestricted use, distribution, and reproduction in any medium, provided the original author and source are credited.

during adolescence [25,26]. Mills and colleagues have illustrated developmental changes across adolescence within a network of social brain regions (medial prefrontal cortex, TPJ, posterior STS, and anterior temporal cortex); however, they did not correlate brain structure with social cognitive skills. In contrast, [25] used a smaller sample at late adolescence but showed that cognitive perspective taking abilities were positively correlated with grey matter volume within the anterior cingulate cortex; and the ability to empathize with fictional characters was positively related to grey matter changes within the right dorsolateral prefrontal cortex.

Therefore, to the best of our knowledge no studies have investigated relations between measures of impulsivity and pro-social behavior based on an inter-temporal choice task and grey matter volume changes estimated by voxel based morphometry (VBM) over the course adolescence. Such studies may facilitate the development of cognitive bio-markers for impulsive and anti-social behavior, and provide predictive approaches to the likely occurrence of impulsivity disorders such as substance abuse or pathological gambling, and/or anti-social behaviors such as aggressiveness, noncompliance, or delinquency.

Materials and Methods

Participants and centers

A large cohort of 298 healthy adolescents [152 males, range: 14-24 years, mean = 19.1 ± 2.9 (SD); 146 females, range: 14-24 years, mean = 19.1 ± 2.9] were scanned over 1½ years at 3 sites: (1) Wellcome Trust Centre for Neuroimaging (WTCN), London, (2) Medical Research Council Cognition and Brain Sciences Unit (MRC CBSU), Cambridge, and (3) Wolfson Brain Imaging Centre (WBIC), Cambridge. The study received ethical approval from the NRES Committee East of England - Cambridge Central (12/EE/0250) and all participants gave written informed consent. This study was conducted by the NeuroScience in Psychiatry Network (NSPN), which addresses how psychiatric disorders are related to abnormal maturation of brain systems.

All cohort members completed cognitive testing and clinical examination with additional behavioral questionnaires. From the original sample of 298 individuals, 26 participants were excluded due to movement artifacts during the structural scanning session; in addition, 59 subjects did not perform well the discounting task and/or the estimation algorithm was not able to fit their behaviors. Despite these issues, we could use 213 healthy adolescents [108 males, range: 14-24 years, mean = 19.3 ± 2.9 (SD); 105 females, range: 14-24 years, mean = 18.8 ± 2.9].

Data acquisition

All multi-parameter maps (MPM) were acquired on 3T whole body MRI systems (Magnetom TIM Trio, Siemens Healthcare, Erlangen, Germany; VB17 software version) operated with the standard 32-channel radio-frequency (RF) receive head coil and RF body coil for transmission. The MPM comprised three multi-echo 3D fast low angle shot (FLASH) scans with PD (TR/α = 23.7 ms/6°), T1 (TR/α = 18.7 ms/20°), and MT (TR/α = 23.7 ms/6°) - weighted contrast, one RF transmit (B_1) field map and one static magnetic (B_0) field map scan [27].

The MPM acquisition and pre-processing were developed and optimized in previous studies and are widely described here [28-33]. The post-processed MT maps resulting from this step were used in our VBM analyses.

The 'Delegated Inter-temporal Discounting' task

As a laboratory measure of impulsivity, a computerized delegated inter-temporal discounting (*DID*) task was used. The *DID* task and the measures that we derived from it had as follows. The task consisted of trials where the participant chose for themselves, and trials where they chose on behalf of an ostensible partner of the same gender and age group. They were informed that at the end of the experiment, one of the trials where they chose for themselves would be randomly selected and the corresponding choice that they made would be paid out to them. In fact during the task participants did not see actual monetary amounts on the screen, but they did see actual time delays. They might, for example, be asked to choose between '100 points today or 150 points in 1 week'. They did not know the exact exchange rate between points and money, but they did know that the task would result in an average payment of £2.50 on top of a flat hourly fee. Importantly, they had no monetary incentive at all to get the answers right for the 'partner'.

In the first 60 trials, the participant chose just for themselves. We interleaved trials selected at random from a broad range [34] and trials that adaptively tracked the discount rate of the participant. The adaptive algorithm assumed that participants made choices according to a hyperbolic discounting function, so that the value difference between an option obtained today and one obtained after a delay D is:

$$\Delta Q = R_{today} - R_{Delayed}/(1/+KD) \quad (1)$$

So that the participant would choose the later (Delayed) option with probability:

$$P_{Delayed} = [1/1+\exp(\Delta Q/T)] \quad (2)$$

The tracking procedure maximized the number of trials that would be maximally informative about the participant's discounting rate. Starting from a prior belief imitating a typical population distribution over K (mean = -2 and SD = 1 in $\log_{10}$ units), we calculated a posterior distribution by updating this belief according to Bayes' rule in the light of each choice the participant made. For the adaptive trials we then selected a pair of options that would be indifferent had the participant's K been at the mode of the posterior. The $\log_{10}$ final estimate of this update procedure, at the 60th trial, was *Kself*.

In the next part of the task, phase 2, the participant had to infer the preferences of a 'partner'. We told participants that the partner was a peer of the same gender using another computer, but in fact it was a hyperbolic-discounting computer agent (as above, except with deterministic policy $T \approx 0$). The *Kother* that was used was drawn as follows:

$$\begin{aligned} &\text{if } Kself > -2 \text{ then} \\ &P(Kother = Kself - 1) \cong 2/3;\ P(Kother = Kself + 1) \cong 1/3 \\ &\text{elseif } Kself \lesssim -2 \text{ then} \\ &P(Kother = Kself - 1) \cong 1/3;\ P(Kother = Kself + 1) \cong 2/3 \end{aligned} \quad (3)$$

That is, *Kother* was always displaced by one $\log_{10}$ unit from *Kself* and this was done more often towards the population mean than away from it (to avoid too many extreme values). The above equalities are approximate because participants who were estimated to have extreme values of discounting were always allocated partners towards the middle of the distribution, again to avoid very extreme values. After each choice 'on behalf of the other', the participant was presented with feedback such as: 'Wrong! [Other's name] chose the other option' etc. We shortened the number of trials in phase 2 if the participant learnt the other's preferences quickly (8 out of 10 correct in the last 10 trials) to save time. The percentage of correct 'chose-for-other' trials in phase 2 is referred to as 'learning performance', *learnPerf*.

In phase 3 of the experiment, blocks of 10 choices-for-self (60 in total) alternated with 10 choices-for-other (another 60), under the same feedback and payment conditions as above. Out of these self-trials we

fitted a new *K* for the self by maximum-likelihood, this time using a flat prior to render it maximally sensitive to changes in *K*. We call this *Kso*. Similarly we computed *K* for the partner, *Kother*.

We then applied a quality-control threshold to the fitting of *Kself*. We only considered participants who had a peak likelihood at least 3 $\log_{10}$ units above the value at either end of the range considered, which was -5 to 0 in $\log_{10}$ units. For the participants that fulfilled this, we then calculated the shift in *K*: *Kshift* = *Kso* – *Kself*. During preliminary analyses we observed that our participants (irrespective of *K*s) tended to shift slightly more towards lower *Kso* others than towards those with higher *Kso*. As Eq. 3, meant that the numbers of these were not balanced, we calculated a first-order correction in *Kother* so that the *Kshift* reported here is as if all participants had partners with lower *Kother* ('more patient'). We wanted *Kshift* to represent how much participants were influenced by learning others' preferences; we therefore expressed *Kshift* by unit *Kself* - *Kother* (as if everyone learnt *Kother* perfectly). Finally, we calculated *Kother* and *Kshift* using not the peak values but the expectations of the relevant likelihood distributions. The reason for doing this is because for some participants the peaks of the relevant distributions no longer fulfilled the quality criterion by the end of phase 3. We will use these two estimated parameters in the structural analyses. The proportion of correct 'chose-for-other' trials in phase 3 is referred to as 'matching performance', *matchPerf*.

We also estimated two measures of variability: *Tself* and *Tsoo*, the softmax temperature parameters for phases 1 (choose-for-self) and 3 (choose-for-other) respectively. This was also done by simple maximum-likelihood estimation, *K* and *T* being fitted together.

Voxel-based morphometry (VBM): Grey matter volume estimates

For VBM analyses, the MT saturation maps were processed in VBM8 (http://dbm.neuro.uni-jena.de/vbm/) with the default settings and classified into different tissue classes: grey matter (GM), white matter (WM), and cerebral-spinal fluid (CSF). The reason for using MT maps is that even though T1w images are commonly used for brain segmentation, the MT maps have been shown to improve the segmentation of subcortical areas [31,35]. Moreover, aiming at optimal anatomical precision we applied the diffeomorphic registration algorithm DARTEL [36]. The warped GM probability maps were scaled by the Jacobian determinants of the deformation fields to account for local compression and expansion, resulting in GM volume (GMV) maps. The GMV maps were then smoothed by convolution with an isotropic Gaussian kernel of 6 mm full-width-at-half-maximum (FWHM).

Statistical analyses

For investigation of correlations of GM volume with age, and discounting estimates, we used paired t-tests with a whole-brain search volume. Regional associations between GM volume, age, and discounting parameters, were then examined by creating voxel-wise statistical parametric maps (SPMs) for the whole-brain volume using the General Linear Model (GLM) and Random Field Theory [37]. Significance level was set at $p < 0.05$ with family-wise error (FWE) correction for multiple comparisons.

Multiple linear regression models

To test the hypotheses that estimated GM volumes are a function of age, discounting estimates, or both, we carried out linear regression analyses.

We first calculated the GM volume maps estimated from MT data. This was followed by a multiple regression analysis explaining GM volume by a constant, age, *Kself*, and age × *Kself*, differentiating between males and females (in order to identify gender-specific effects), scanner site, and total intracranial volume. The correlation was modeled as:

$$GMV = \beta_1 \times [\text{constant}_{\text{male}}] + \beta_2 \times [\text{age}_{\text{male}}] + \beta_3 \times [\text{Kself}_{\text{male}}] + \beta_4 \times [\text{age}_{\text{male}} \times \text{Kself}_{\text{male}}] + \beta_5 \times [\text{constant}_{\text{female}}] + \beta_6 \times [\text{age}_{\text{female}}] + \beta_7 \times [\text{Kself}_{\text{female}}] + \beta_8 \times [\text{age}_{\text{female}} \times \text{Kself}_{\text{female}}] + \beta_9 \times [\text{site}] + \beta_{10} \times [\text{TICV}] \quad (4)$$

All independent variables in Eq. (4) were mean corrected. This multiple linear regression was performed on a voxel-by-voxel basis beyond the statistical threshold $p_{FWE} < 0.05$ in the paired t-test of interest. However, for the illustration of the results, we will show statistical maps thresholded at $p < 0.001$ uncorrected (see Results section).

$$GMV = \beta_1 \times [\text{constant}_{\text{male}}] + \beta_2 \times [\text{age}_{\text{male}}] + \beta_3 \times [\text{Kself}_{\text{male}}] + \beta_4 \times [\text{age}_{\text{male}} \times \text{Kself}_{\text{male}}] + \beta_5 \times [\text{constant}_{\text{female}}] + \beta_6 \times [\text{age}_{\text{female}}] + \beta_7 \times [\text{Kself}_{\text{female}}] + \beta_8 \times [\text{age}_{\text{female}} \times \text{Kself}_{\text{female}}] + \beta_9 \times [\text{site}] + \beta_{10} \times [\text{TICV}]$$

We then considered the same correlation model for the rest of the discounting parameters. The reason for doing this is that some of the parameters were highly correlated (i.e., between *Kself* and *Tself*, Pearson-correlation = 0.64 in males, and 0.58 in females). For instance, the correlation model for the temperature parameter: *Tself*, can be re-written as:

$$GMV = \beta_1 \times [\text{constant}_{\text{male}}] + \beta_2 \times [\text{age}_{\text{male}}] + \beta_3 \times [\text{Tself}_{\text{male}}] + \beta_4 \times [\text{age}_{\text{male}} \times \text{Tself}_{\text{male}}] + \beta_5 \times [\text{constant}_{\text{female}}] + \beta_6 \times [\text{age}_{\text{female}}] + \beta_7 \times [\text{Tself}_{\text{female}}] + \beta_8 \times [\text{age}_{\text{female}} \times \text{Tself}_{\text{female}}] + \beta_9 \times [\text{site}] + \beta_{10} \times [\text{TICV}] \quad (5)$$

Unfortunately, only two more cognitive parameters: *Tself* and *Kshift*, achieved whole-brain significance level. For the sake of simplicity we will show the correlation maps of the significant estimates.

Results

We used grey matter volume estimates for examining correlations with age and discounting parameters. A subset of three cognitive parameters: *Kself*, *Tself*, and *Kshift*, reached whole-brain significance level.

Figure 1 shows the correlation map between GMV and age. Overall,

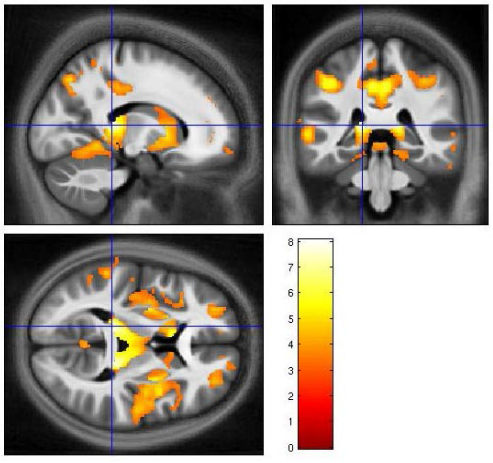

Figure 1: Negative correlation of age and grey matter volume (GMV). Statistical map thresholded at $p < 0.001$ (unc.) showing brain areas negatively correlated with age. Analysis revealed the maximum correlation within left thalamus (peak coordinate: (-14, -34, 9), $p < 0.05$, whole-brain FWE-corrected at the peak-level). In addition, other brain areas such as middle cingulate, midbrain, bilateral inferior parietal lobule, bilateral middle temporal gyrus, bilateral striatum, and bilateral dorsolateral prefrontal cortex (DLPFC), also showed a significant correlation.

we observed an age dependent global decrease in grey matter volume over the brain throughout adolescence.

Interestingly, we observed a relationship between our measure of self-discounting and the trajectory of morphological brain changes. Figure 2 illustrates the correlation map between GMV and *Kself*. Specifically, the higher the self-discounting parameter (the more impulsive adolescents behaved in the task, evidenced in a propensity to accept the sooner smaller over the larger later option) and older, the greater the grey matter volume within right dorsomedial prefrontal cortex (DMPFC).

We also observed that the higher the decision-variability parameter (the more "noisy" and "exploratory" adolescents behaved) and older, the higher was the grey matter volume within bilateral dorsal striatal aspects. Figure 3 shows their corresponding correlation map.

Finally, we observed that a higher *Kshift* (the more malleable individuals were prone to change towards other's behavior), the higher was the grey matter volume within right dorsolateral prefrontal cortex (DLPFC). Figure 4 illustrates the correlation map.

Discussion

In this study, we used a large cohort of healthy male and female participants aged 14-24 years measured using structural magnetic resonance imaging (MRI) techniques (N=213). All MRI cohort members completed cognitive testing and a clinical examination with additional behavioral questionnaires. Our primary goal was to understand neurobiological mechanisms underlying impulsive and pro-social behaviors by studying associations between cognitive parameters derived from a discounting task and grey matter volume estimated by voxel based morphometry (VBM).

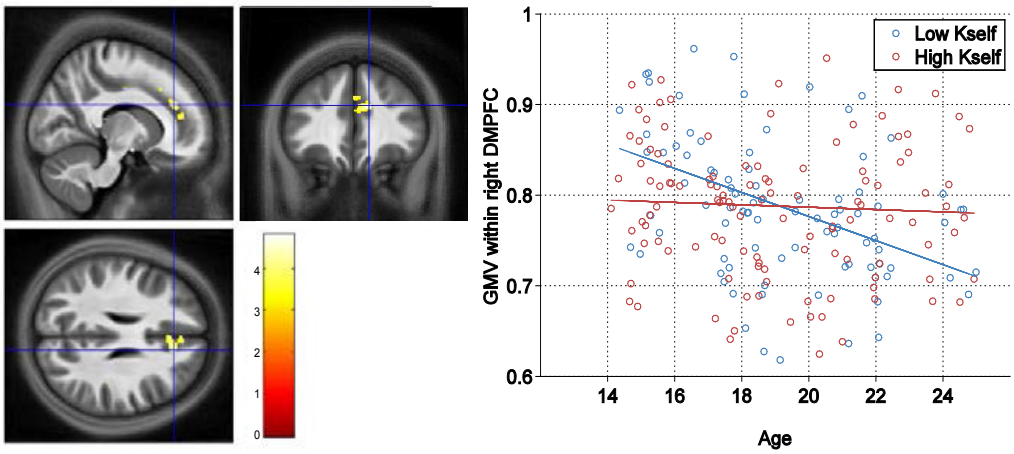

Figure 2: Positive correlation of age × *Kself* and grey matter volume (GMV) within right dorsomedial prefrontal cortex (DMPFC).

A. Statistical map thresholded at $p < 0.001$ (unc.) showing brain areas positively correlated with age × *Kself*. Analysis revealed the maximum correlation within right DMPFC (peak coordinate: (12,35, 25), $p < 0.05$, whole-brain FWE-corrected at the peak-level). **B.** Linear regression of GMV within right DMPFC on age differentiating low- vs. high-*Kself* individuals. Low-*Kself* participants show a decrease of GMV within right DMPFC aspects as they get older, whereas high-*Kself* individuals do not show any decrease of GMV within right DMPFC aspects.

**Plotted GMV estimates were extracted from the cluster around the peak-voxel at: (12,35,25).*

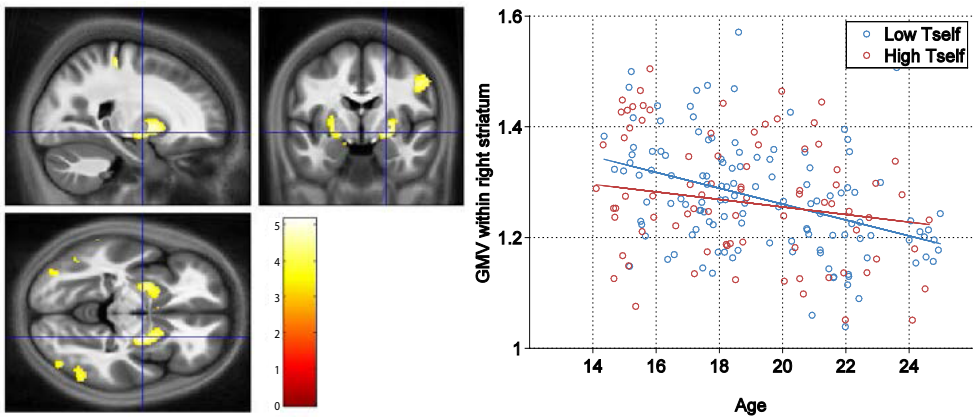

Figure 3: Positive correlation between age × *Tself* and grey matter volume (GMV) within right dorsal striatum.

A. Statistical map thresholded at $p < 0.001$ (unc.) showing brain areas positively correlated with age × *Tself*. Analysis revealed the maximum correlation within right dorsal striatum (peak coordinate: (22,-4, -6), $p < 0.05$, whole-brain FWE-corrected at the peak-level). **B.** Linear regression of GMV within right dorsal striatum on age differentiating low-vs. high-*Tself* individuals. Low *Tself* participants show a stronger decrease of GMV within right dorsal striatum as they get older, whereas high-*Tself* individuals show a weaker decrease of GMV within right dorsal striatum.

**Plotted GMV estimates were extracted from the cluster around the peak-voxel at: (22,-4 -6).*

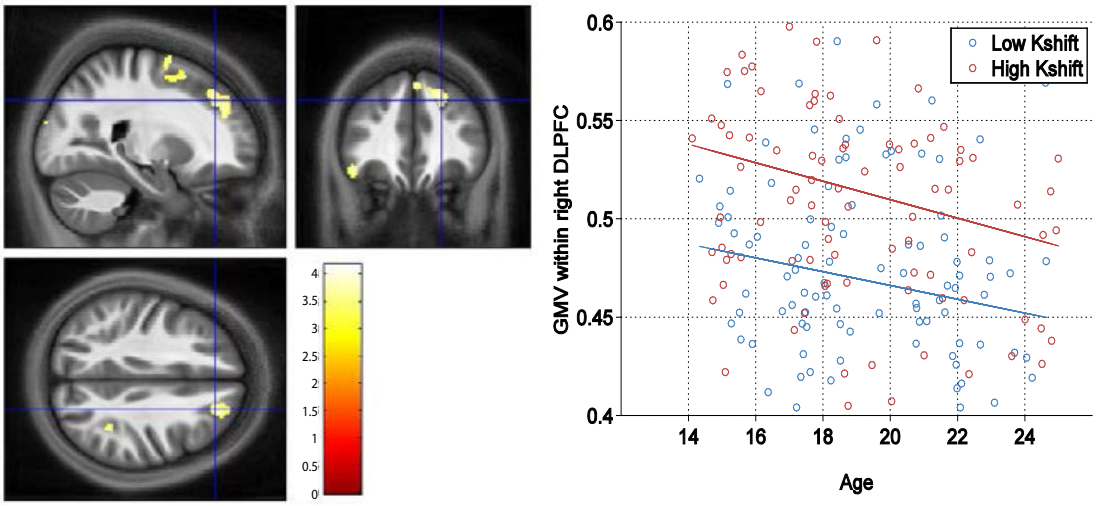

Figure 4: Positive correlation between *Kshift* and grey matter volume (GMV) within right dorsolateral prefrontal cortex (DLPFC).

A. Statistical map thresholded at p < 0.001 (unc.) showing brain areas positively correlated with *Kshift*. Analysis revealed the maximum correlation within right DLPFC (peak coordinate at: (22,36,37), p < 0.05, whole-brain FWE-corrected at the cluster-level). **B.** Linear regression of GMV within right DLPFC on age differentiating low- vs. high-*Kshift* individuals. Both low-and high-*Kshift* individuals show a decrease of GMV within right DLPFC as they get older. Thus, the more they shift towards the other, no matter whether they are younger or older, the greater the grey matter volume within right DLPFC.

** Plotted GMV estimates were extracted from the cluster around the peak-voxel at: (22,36,37).*

*** Kshift defined as (Kself-other–Kself) × direction (Kother)*

Overall we observed a global decrease in grey matter volume over the course of adolescence. This result replicates previous studies with increasingly large groups of participants [38,39]. Over and above these changes greater impulsivity as indexed in a higher self-discounting parameter was linked to greater grey matter volume within right DMPFC. Likewise we observed that greater choice stochasticity, indexed by a higher decision-variability parameter was linked to greater grey matter volume within bilateral dorsal striatum.

These impulsivity-related findings may indicate that a delay in cortical maturation, i.e. a sluggish brain pruning process during adolescence development, within brain regions implicated in decision making is a key mediator of impulsivity. Adolescents having impulsive behaviors while performing a discounting task (indexed by high self-discounting and decision-variability parameters), might have a deficient pruning process resulting in a surplus of brain synapses, i.e. greater grey matter volumes, within DMPFC aspects and dorsal striatal areas.

Synapses are known to be affected by many genes linked to psychiatric disorders, and some colleagues have already demonstrated that boys with conduct disorders may have more synapses [40,41]. Indeed the regions of the cortex which undergo the most pruning during adolescence are the ones we most associate with teenage behavior, e.g. impulsive traits. Our results are consistent with the literature [42] and we do believe that the shrinkage of the grey matter is due to a very complex and well-organized mechanism restructuring child's brain. Therefore, abnormalities in this pruning process may explain the finding that most of the major psychiatric disorders - of thought, mood, and anxiety - have their major onset during this vulnerable period.

Finally, the ability to shift towards other's behavior was positively correlated to grey matter volume within right DLPFC. This pro-social-related finding suggests that the capacity to change towards other's behavior requires of a greater grey matter volume within DLPFC aspects. At first glance, this result seems to contradict previous impulsitivity-related findings but actually it does not. Overall we observed a global decrease in grey matter volume over the brain and indeed, the DLPFC also undergo a normal pruning process over the course of adolescence (Figure 1). In essence, what this result says is that the more grey matter you have got at the onset of puberty, the more malleable you are in shifting towards other's behaviour. It must be stressed that this trait seems to be already implemented at the beginning of adolescence. Notice that the two curves run parallel along the *x* axis (i.e. the 'age' axis) and the distance between them stays constant highlighting the fact that this effect can be purely described by the intercept (Figure 4).

This finding supports the idea that pro-social traits may be developed early in time, during childhood. Children's personality traits have enduring effects that shape adult behavior and childhood experiences influences core aspects of adult well-being. Indeed, current research is now examining the mechanisms by which early personality traits initiate and sustain particular life paths [43-45]. Therefore, our finding suggests that the ability to follow other's actions might initiate in childhood and follows a mechanism that last throughout adolescence.

In summary, our findings are suggestive of grey matter volume within right DMPFC and bilateral striatal aspects as potential biological markers for impulsivity-related traits over the course of adolescence that may have diagnostic and predictive utility. Moreover, they also suggest grey matter volume within right DLPFC as a plausible marker for pro-social-related traits over the course of childhood, as it seems that this trait is already formed at the onset of puberty.

Acknowledgements

This work was funded by grants from the Wellcome Trust. Authors acknowledge support by NSPN (NeuroScience in Psychiatry Network) Principals, NSPN Research Assistant team, NSPN Data Management team, and U-CHANGE (Understanding & Characterizing Adolescent-to-Adult Neurdvelopmental Growth Effects) team. D. Bernal-Casas wishes to thanks relatives and friends for their continued moral and financial support.

References

1. Blakemore SJ, Choudhury S (2006) Brain development during puberty: state of the science. Dev Sci 9: 11-14.
2. Casey BJ, Getz S, Galvan A (2008) The adolescent brain. Dev Rev 28: 62-77.
3. Bjork JM, Momenan R, Hommer DW (2009) Delay discounting correlates with proportional lateral frontal cortex volumes. Biol Psychiatry 65: 710-713.
4. Boes AD, Bechara A, Tranel D, Anderson SW, Richman L, et al. (2009) Right ventromedial prefrontal cortex: a neuroanatomical correlate of impulse control in boys. Soc Cogn Affect Neurosci 4: 1-9.
5. Cho SS, Pellecchia G, Aminian K, Ray N, Segura B, et al. (2013) Morphometric correlation of impulsivity in medial prefrontal cortex. Brain Topogr 26: 479-487.
6. Matsuo K, Nicoletti M, Nemoto K, Hatch JP, Peluso MA, et al. (2009) A voxel-based morphometry study of frontal gray matter correlates of impulsivity. Hum Brain Mapp 30: 1188-1195.
7. Dolan RJ, Dayan P (2013) Goals and habits in the brain. Neuron 80: 312-325.
8. Bissonette GB, Burton AC, Gentry RN, Goldstein BL, Hearn TN, et al. (2013) Separate populations of neurons in ventral striatum encode value and motivation. PLoS One 8: e64673.
9. Sescousse G, Li Y, Dreher JC (2015) A common currency for the computation of motivational values in the human striatum. Soc Cogn Affect Neurosci 10: 467-473.
10. Tricomi E, Balleine BW, O'Doherty JP (2009) A specific role for posterior dorsolateral striatum in human habit learning. Eur J Neurosci 29: 2225-2232.
11. Yin HH, Knowlton BJ, Balleine BW (2004) Lesions of dorsolateral striatum preserve outcome expectancy but disrupt habit formation in instrumental learning. Eur J Neurosci 19: 181-189.
12. de Wit S, Corlett PR, Aitken MR, Dickinson A, Fletcher PC (2009) Differential engagement of the ventromedial prefrontal cortex by goal-directed and habitual behavior toward food pictures in humans. J Neurosci 29: 11330-11338.
13. Levy DJ, Glimcher PW (2012) The root of all value: a neural common currency for choice. Curr Opin Neurobiol 22: 1027-1038.
14. Valentin VV, Dickinson A, O'Doherty JP (2007) Determining the neural substrates of goal-directed learning in the human brain. J Neurosci 27: 4019-4026.
15. Gill TM, Castaneda PJ, Janak PH (2010) Dissociable roles of the medial prefrontal cortex and nucleus accumbens core in goal-directed actions for differential reward magnitude. Cereb Cortex 20: 2884-2899.
16. Mitchell DG, Luo Q, Avny SB, Kasprzycki T, Gupta K, et al. (2009) Adapting to dynamic stimulus-response values: differential contributions of inferior frontal, dorsomedial, and dorsolateral regions of prefrontal cortex to decision making. J Neurosci 29: 10827-10834.
17. Warden MR, Selimbeyoglu A, Mirzabekov JJ, Lo M, Thompson KR, et al. (2012) A prefrontal cortex-brainstem neuronal projection that controls response to behavioural challenge. Nature 492: 428-432.
18. Decety J, Lamm C (2006) Human empathy through the lens of social neuroscience. ScientificWorldJournal 6: 1146-1163.
19. Preston SD, de Waal FB (2002) Empathy: Its ultimate and proximate bases. Behav Brain Sci 25: 1-20.
20. Frith U, Frith CD (2003) Development and neurophysiology of mentalizing. Philos Trans R Soc Lond B Biol Sci 358: 459-473.
21. Samson D, Apperly IA, Chiavarino C, Humphreys GW (2004) Left temporoparietal junction is necessary for representing someone else's belief. Nat Neurosci 7: 499-500.
22. Saxe R, Kanwisher N (2003) People thinking about thinking people. The role of the temporo-parietal junction in "theory of mind". Neuroimage 19: 1835-1842.
23. Sebastian CL, Fontaine NM, Bird G, Blakemore SJ, Brito SA, et al. (2012) Neural processing associated with cognitive and affective Theory of Mind in adolescents and adults. Soc Cogn Affect Neurosci 7: 53-63.
24. Schnell K, Bluschke S, Konradt B, Walter H (2011) Functional relations of empathy and mentalizing: an fMRI study on the neural basis of cognitive empathy. Neuroimage 54: 1743-1754.
25. Banissy MJ, Kanai R, Walsh V, Rees G (2012) Inter-individual differences in empathy are reflected in human brain structure. Neuroimage 62: 2034-2039.
26. Mills KL, Lalonde F, Clasen LS, Giedd JN, Blakemore SJ (2014) Developmental changes in the structure of the social brain in late childhood and adolescence. Soc Cogn Affect Neurosci 9: 123-131.
27. Weiskopf N, Lutti A, Helms G, Novak M, Ashburner J, et al. (2011) Unified segmentation based correction of R1 brain maps for RF transmit field inhomogeneities (UNICORT). Neuroimage 54: 2116-2124.
28. Helms G, Dathe H, Dechent P (2008) Quantitative FLASH MRI at 3T using a rational approximation of the Ernst equation. Magn Reson Med 59: 667-672.
29. Helms G, Dathe H, Kallenberg K, Dechent P (2008) High-resolution maps of magnetization transfer with inherent correction for RF inhomogeneity and T1 relaxation obtained from 3D FLASH MRI. Magn Reson Med 60: 1396-1407.
30. Helms G, Dathe H, Weiskopf N, Dechent P (2011) Identification of signal bias in the variable flip angle method by linear display of the algebraic Ernst equation. Magn Reson Med 66: 669-677.
31. Helms G, Draganski B, Frackowiak R, Ashburner J, Weiskopf N (2009) Improved segmentation of deep brain grey matter structures using magnetization transfer (MT) parameter maps. Neuroimage 47: 194-198.
32. Lutti A, Hutton C, Finsterbusch J, Helms G, Weiskopf N (2010) Optimization and validation of methods for mapping of the radiofrequency transmit field at 3T. Magn Reson Med 64: 229-238.
33. Lutti A, Stadler J, Josephs O, Windischberger C, Speck O, et al. (2012) Robust and fast whole brain mapping of the RF transmit field B1 at 7T. PLoS One 7: e32379.
34. Tardif CL, Collins DL, Pike GB (2009) Sensitivity of voxel-based morphometry analysis to choice of imaging protocol at 3 T. Neuroimage 44: 827-838.
35. Ashburner J (2007) A fast diffeomorphic image registration algorithm. Neuroimage 38: 95-113.
36. Yushkevich PA, Detre JA, Mechanic-Hamilton D, Fernández-Seara MA, Tang KZ, et al. (2007) Hippocampus-specific fMRI group activation analysis using the continuous medial representation. Neuroimage 35: 1516-1530.
37. Giedd JN, Blumenthal J, Jeffries NO, Castellanos FX, Liu H, et al. (1999) Brain development during childhood and adolescence: a longitudinal MRI study. Nat Neurosci 2: 861-863.
38. Pfefferbaum A, Mathalon DH, Sullivan EV, Rawles JM, Zipursky RB, et al. (1994) A quantitative magnetic resonance imaging study of changes in brain morphology from infancy to late adulthood. Arch Neurol 51: 874-887.
39. Sowell ER, Peterson BS, Thompson PM, Welcome SE, Henkenius AL, et al. (2003) Mapping cortical change across the human life span. Nat Neurosci 6: 309-315.
40. De Brito SA, Mechelli A, Wilke M, Laurens KR, Jones AP, et al. (2009) Size matters: increased grey matter in boys with conduct problems and callous-unemotional traits. Brain 132: 843-852.
41. Dumontheil I, Houlton R, Christoff K, Blakemore SJ (2010) Development of relational reasoning during adolescence. Dev Sci 13: F15-24.
42. Hampson SE, Goldberg LR, Vogt TM, Dubanoski JP (2007) Mechanisms by which childhood personality traits influence adult health status: educational attainment and healthy behaviors. Health Psychol 26: 121-125.
43. Nave CS, Sherman RA, Funder DC, Hampson SE, Goldberg LR (2010) On the Contextual Independence of Personality: Teachers' Assessments Predict Directly Observed Behavior after Four Decades. Soc Psychol Personal Sci 3: 1-9.
44. Soto CJ, John OP (2014) Traits in transition: the structure of parent-reported personality traits from early childhood to early adulthood. J Pers 82: 182-199.
45. Nicolle A, Klein-Flügge MC, Hunt LT, Vlaev I, Dolan RJ, et al. (2012) An agent independent axis for executed and modeled choice in medial prefrontal cortex. Neuron 75: 1114-1121.